

CRC-RL: A Novel Visual Feature Representation Architecture for Unsupervised Reinforcement Learning

Darshita Jain¹, Anima Majumder¹, Samrat Dutta¹, Swagat Kumar²

¹ TATA Consultancy Services, Bangalore, India.

² Edge Hill University, UK.

March 2, 2023

¹(darshita.jain, anima.majumder, d.samrat)@tcs.com , ² kumars@edgehill.ac.uk

Abstract

This paper addresses the problem of visual feature representation learning with an aim to improve the performance of end-to-end reinforcement learning (RL) models. Specifically, a novel architecture is proposed that uses a heterogeneous loss function, called CRC loss, to learn improved visual features which can then be used for policy learning in RL. The CRC-loss function is a combination of three individual loss functions, namely, contrastive, reconstruction and consistency loss. The feature representation is learned in parallel to the policy learning while sharing the weight updates through a Siamese Twin encoder model. This encoder model is augmented with a decoder network and a feature projection network to facilitate computation of the above loss components. Through empirical analysis involving latent feature visualization, an attempt is made to provide an insight into the role played by this loss function in learning new action-dependent features and how they are linked to the complexity of the problems being solved. The proposed architecture, called CRC-RL, is shown to outperform the existing state-of-the-art methods on the challenging Deep mind control suite environments by a significant margin thereby creating a new benchmark in this field.

In the recent past, deep reinforcement learning (DRL) algorithms have been successfully used to learn action policies directly from visual observations, thereby finding application in several interesting areas such as gaming [1, 2], robotics [3, 4, 5, 6] and autonomous vehicles [7, 8] etc. This success is mostly driven by the agent's ability to jointly learn feature representation and policy decisions by using long-term credit-assignment capabilities of reinforcement learning algorithms in an end-to-end fashion. In spite of this success, RL algorithms are known to be sample-inefficient

and suffer from poor generalization for high-dimensional observations such as images [9, 10]. There are several approaches to address these concerns, including methods such as, transfer learning [11, 12], meta-learning [13] [14] and active learning [15]. *Feature representation learning* [16] is an alternative, and sometimes complementary, to these approaches which aims at learning useful features that can simplify the intended task, e.g., classification or prediction. This paper primarily focuses on this later approach as it is now widely accepted that the problem of sample-inefficiency in RL can be solved to a great extent by learning suitable feature representation which is shown to expedite the policy learning process [17]. The feature representations are learned using self-supervised methods which are increasingly becoming popular as they obviate the need for manually generated labeled datasets thereby simplifying the practical deployment of deep learning models [18]. Some of these approaches include auto-encoders [19], GANs [20] [21], contrastive learning [22] and data augmentation techniques [9] [23]. The features thus obtained have been shown to greatly improve the sample efficiency and generalizability of RL methods as demonstrated in [24] [10] [23].

Rather than decoupling the representation learning from policy learning as done in [25] [23] [17], we continue working with end-to-end models because of their simplicity and aim at improving their performance by performing auxiliary tasks as demonstrated in [10] [26]. Since the feature representations are learned along side the policy decisions in an end-to-end fashion, the features learned are actually *action-dependent*. This is because, the backward gradient flow from the policy-learning algorithm is allowed to update the encoder weights. This makes the learned feature vectors strongly correlated to the actions being taken by the agent [27]. Given this hindsight, we are motivated by two factors. First, it is our belief that the quality of the fea-

tures learnt could be improved by using a better loss function leading to improved RL performance. Secondly, we are keen to develop a better understanding of the relationship between the feature and action spaces. Towards fulfilling these objectives, we propose a new heterogeneous loss function called *CRC loss* for feature representation learning by combining three different loss functions, namely, *contrastive loss* [10], *reconstruction loss* and *consistency loss*. The reconstruction loss obtained with an auto-encoder model helps in learning compact features that is sufficient to reconstruct the original observations. On the other hand, the consistency loss [23] helps in learning features that are invariant to image augmentations. In other words, by minimizing the consistency loss, the encoder is encouraged to learn *task-relevant* features while ignoring irrelevant aspects (such as, background color) thereby avoiding observational over-fitting [28]. Similarly, the contrastive loss helps in learning *class-invariant* features from augmented images by contrasting them against a batch of negative samples. In that sense, these three loss functions contribute complementary information and hence, should improve the feature representation learning when combined together. In order to implement feature training with this loss function, a new architecture inspired by CURL [10], is proposed that uses a Siamese Twin encoder model, a decoder network and a feature predictor to generate these losses. Through empirical analysis including feature visualizations, it is shown that the feature representations learnt by the CRC loss function is different from those learnt with the baseline CURL model, indicating the role played by the CRC-loss in learning new action-dependent features. In addition, visualization of correlation matrices between latent features generated by this model show increasingly complex patterns for complex environments with higher-dimensional action spaces, thereby providing a clue about how features are inherently linked with action in an end-to-end RL model. Through rigorous experiments on the challenging Deep Mind Control suite environments [29], it is shown that the proposed CRC-RL model outperforms the existing state-of-the-art methods by a significant margin, thereby establishing the efficacy of the approach. The design choices for the proposed model are justified through extensive ablation studies.

In short, the major contributions made in this paper are as follows:

1. A new self-supervised feature representation architecture along with a novel loss function is proposed to improve the performance of RL models in learning policies directly from image observations.
2. Through empirical analysis involving latent feature visualization, an attempt has been made to provide insights into the relationship between the action and feature space thereby providing better standing of the role

played of the new loss function in learning *action-dependent* features.

3. The resulting architecture is shown to outperform existing state-of-the-art methods on the challenging DMC environments by a significant margin.

The rest of this paper is organized as follows. Related works are reviewed in the next section. The proposed architecture is described in Section 2. The experimental results are discussed and analyzed in Section 3. The paper ends with the concluding section 4.

1 Related Works

This section provides an overview of related literature in the following subsections.

1.1 Deep RL architectures for policy learning

Reinforcement learning algorithms learn the optimal policy for a given task by maximizing a measure of *cumulative discounted future reward* for the task while balancing between *exploration* (of new possibilities) and *exploitation* (of past experiences) [30]. This cumulative discounted reward function, represented as Q or *value* function, is not known a priori and, is used to evaluate a given action taken by the agent. Depending on how this function is estimated and desirable actions are derived from it, the RL-based methods can be broadly classified into two categories: *value-based* methods and *policy-based methods*. The value-based methods aim at estimating the Q-function and then derive action from this by using a greedy policy. On the other hand, policy-based methods directly estimate the policy function by maximizing a given objective function. The traditional Q-learning algorithm estimates the Q function iteratively by using an approximate dynamic programming formulation based on Bellman’s equation starting from an initial estimate [31]. The original Q-learning algorithm could be applied to problems with discrete state (observation) and action spaces and hence, suffered from the *curse-of-dimensionality* problem with higher dimensions and range of values. This limitation is overcome by using a deep network to estimate Q function that can take arbitrary observation inputs, thereby, greatly enhancing the capabilities of RL algorithms. The resulting approach is known as Deep Q Networks (DQN) [32] [33] which has been applied successfully to a wide range of problems while achieving superhuman level performances in a few cases, such as ATARI video games [34], Go [35] etc. The success of DQN has spawned a new research field known as deep reinforcement learning (DRL) attracting a large following of researchers. Readers are referred to [36] for a survey of this field. The DQN models were subsequently extended

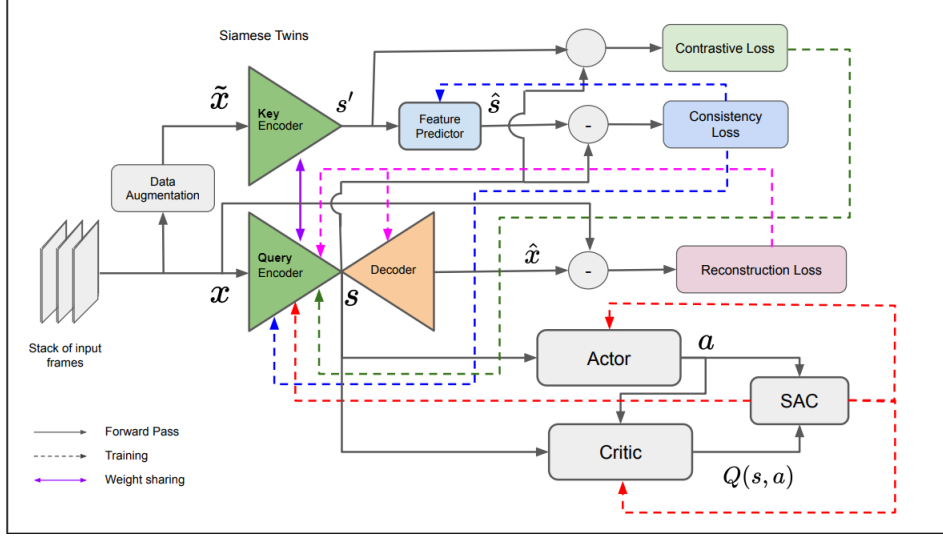


Figure 1: CRC-RL Architecture: It consists of a Siamese Twin encoder along with a decoder and a feature predictor network. The query encoder together with the decoder forms an auto-encoder. The query encoder is used for learning policy using SAC algorithm. Observations are data-augmented to form query and key observations, which are then encoded into latent features by the respective encoders. Only the query encoder weights are updated during the training step. The weights of key encoder are exponential moving average of query encoder weights.

to continuous action spaces by using policy gradient methods that used a parameterized policy function to maximize DQN output using gradient ascent methods [37] [38]. This has opened the doors for solving various robotics problems that use continuous values such as joint angles, joint velocities or motor torques as input. Since then, a number of methods have been proposed to improve the performance of RL algorithms and have been applied successfully to different robotic problems - manipulation [39] [40], grasping [41] [42], navigation [43] etc. Some of the notable methods include actor-critic models - A2C and A3C [44], soft actor-critic (SAC) [45] and proximal policy optimization (PPO) [46]. In spite of the success of these methods, (deep) reinforcement learning algorithms, in general, suffer from limitations such as poor sampling efficiency leading to longer training time, poor generalization and instability. The work presented in this paper aims to address some of these concerns by focusing on learning better task-relevant features.

1.2 Feature Representation Learning in RL

It is now widely accepted that learning policies from low-dimensional feature vectors based on physical states is much more sample efficient compared to learning directly from image pixels [10] [47]. Hence, it is imperative to learn suitable state representations from image observations that will reduce the search space thereby improving the sample efficiency and stability of RL algorithms. The field of self-supervised representation learning has seen great progress in last few years. Auto-encoders [19] [48] learn the state representation by compressing the observa-

tion into low-dimensional state that is sufficient to reconstruct the observation. These have been used to improve the performance of RL algorithms as demonstrated in [17][49] [50] [24]. On the other hand, contrastive learning [22] [51] learns the class-relevant feature representations by maximizing the agreement between the augmented versions of the same observation. It has been shown to greatly improve the sample efficiency of RL algorithms as in [10]. Similarly, recent studies have shown that the right kind of data augmentation techniques can improve the sample efficiency and generalization capabilities of RL algorithms learning *task-relevant* features which remain unaffected by distractions introduced by the augmentation [9] [52]. This can be further enforced by making the encoder minimize the consistency loss as suggested in [23]. In short, learning suitable feature representation plays a significant role in improving the performance of RL algorithms by increasing sample efficiency, improving generalization and stability. The work presented in this paper contributes to this field by proposing a novel loss function that leads to superior learning performance for continuous control tasks as will be demonstrated later in this paper.

2 Method

This section provides details of the proposed CRC-RL model that uses a novel heterogeneous loss function to extract useful information from visual images to be used for learning optimal policy using an end-to-end RL framework. The discussion is organized in the following subsections.

The architecture of the proposed model is described next.

2.1 The Model Architecture

The overall architecture of the proposed model is shown in Figure 1. The observation is available in the form of images which are stacked together to act as input to the model. Stacking of frames is a heuristic approach to incorporate temporal information in the learning process [53]. The observations obtained from the environment is stored in a replay buffer \mathcal{D} and a batch is sampled from this replay buffer during the training process. A Siamese Twin encoder model is employed for extracting features from the input images. These two encoders, termed as *query* and *key* encoders, are used for computing contrastive and consistency losses. The query encoder with a decoder is used for computing the reconstruction loss. A combination of these three losses, known as the CRC loss, is used for updating the parameters of the query encoder and decoder network. The input images are augmented before applying to the key encoder. The features obtained from the query encoder is used for policy estimation using soft-actor-critic algorithm [45]. The parameters of the query encoder and decoder networks are updated using error signals obtained from their own outputs as well as from the RL algorithm. Since the encoder networks are getting influenced by the RL policy algorithm, the features learnt in the process are *action-dependent*. This aspect will be analyzed in more detail in the experiment section presented later in this paper. The weights of the key encoder network is the exponential moving average of the query encoder weights. The proposed CRC loss function used for learning the feature embeddings is discussed in the next subsection.

2.2 The loss function for feature extraction

The query encoder is trained using the proposed CRC loss function which is a combination of the following three loss components as described below.

2.2.1 Contrastive loss

In contrastive learning, we have a query q observation and a set of key observation samples $\mathbb{K} = \{k_0, k_1, \dots\}$ consisting of both positive samples (k_+) and negative samples ($\mathbb{K} \setminus k_+$). The positive samples are those that belong to the same class as that of the query observation and the rest are considered to be the negative samples. The goal is to learn embeddings such that q is relatively more similar to the positive keys k_+ than the negative keys in the latent space. The query and key observations, generated by applying data augmentation on sampled observations, are encoded using the query and key encoder respectively. The contrastive loss

depends on the output of both the encoders (Siamese Twin) represented by the symbols \mathbf{s} and \mathbf{s}' respectively. The idea behind using the contrastive loss is that the different augmentations of the same image will have the same underlying information and hence their high-level representations will be mapped together in the latent space. The similarity between the query and the key embeddings is computed using the bilinear inner-product $q^T W k > 0$ where W is a symmetric matrix of parameters to be estimated [54] along with other parameters during the training process. The objective of training is to reduce this similarity measure so that the query embeddings become more distinct from the key embeddings over time ($q^T W k \approx 0 \Rightarrow q \perp k, W > 0$). This is achieved by minimizing the InfoNCE loss [55] given by:

$$L_q = \log \frac{\exp(q^T W k_+)}{\sum_{k_i \in \mathbb{K}} \exp(q^T W k_i)} \quad (1)$$

2.2.2 Reconstruction loss

A well-trained encoder-decoder network is expected to reconstruct the input image at the output of the decoder network. The reconstruction loss is computed based on the inaccuracy in the reconstructed image. A convolutional encoder f_θ maps an input observation $\mathbf{x} \in \mathbb{R}^{m \times n \times 3}$ to a lower-dimensional latent vector $\mathbf{s} \in \mathbb{R}^l$, and a deconvolutional decoder g_ϕ then reconstructs \mathbf{s} back to $\hat{\mathbf{x}} \in \mathbb{R}^{m \times n \times 3}$ such that

$$f_\theta : \mathbf{x} \rightarrow \mathbf{s} \quad (2)$$

$$g_\phi : \mathbf{s} \rightarrow \hat{\mathbf{x}} \quad (3)$$

Both the encoders and decoder are trained simultaneously by maximizing the expected log-likelihood. The reconstruction loss checks how well the image has been reconstructed from the input. The reconstruction loss forces the update such that the latent representation preserves the core attributes of the input data. An L_2 penalty is imposed on the learned representation \mathbf{s} and a weight-decay is imposed on the decoder parameters to incorporate the regularization affects as proposed in [56].

$$L_r = \mathbb{E}_{\mathbf{x} \sim D} [\log p_\theta(\mathbf{x}|\mathbf{s}) + \lambda_s \|\mathbf{s}\|^2 + \lambda_\theta \|\theta\|^2] \quad (4)$$

where λ_s , and λ_θ are hyper-parameters.

2.2.3 Consistency loss

The consistency loss depends on the output of both the query and key encoder f_θ and f'_θ . Here, the query encoder takes the original non-augmented observation \mathbf{x} and the key encoder uses the augmented observation $\tilde{\mathbf{x}}$ as input. The output of the Key encoder \mathbf{s}' is then used as an input to a feature predictor module, which is nothing but an MLP, to estimate the non-augmented embedding $\hat{\mathbf{s}}$. The

consistency loss is designed to minimize the error between the non-augmented embedding \mathbf{s} and the augmented embedding \mathbf{s}' , thereby enabling the encoder to learn essential *task-relevant* features while ignoring irrelevant distractions (such as background clutter or texture). This eliminates the need of using negative samples for the computation of consistency loss. The consistency loss function can, therefore, be mathematically written as:

$$L_c(\hat{\mathbf{s}}, \mathbf{s}, \theta) = \mathbb{E}_{\mathbf{x} \sim \mathcal{D}} [\|\hat{\mathbf{s}} - \mathbf{s}\|^2] \quad (5)$$

2.3 The CRC loss function

It is our conjecture that each of the above three loss functions enables the encoder to extract non-redundant and complementary information from the higher dimensional input. Thus, a combination of these three should improve the overall RL performance in learning optimum policy. The resulting loss function, called CRC loss, has the following mathematical form:

$$L_{CRC} = c_1 L_q + c_2 L_r + c_3 L_c \quad (6)$$

where $c_i > 0$, $\sum_i c_i = 1$, $i = 1, 2, 3$ are hyper-parameters that control the relative importance of individual components. The RL model for policy learning takes the query encoder output as its input. The SAC algorithm used for learning policy is also allowed to affect the query encoder weights f_θ during the backward gradient update step. At regular intervals, the key encoder f'_θ weights are updated using the exponential moving average (EMA) of the weights of the query encoder f_θ . The feature learning and policy learning takes place in jointly in parallel. The latent representations learned by the query encoder f_θ receives gradients from both the CRC loss and the SAC algorithm losses. This makes the feature representations *action-dependent*, an aspect which will be analyzed in some more detail in the next section.

3 Experimental Results and Discussions

The proposed CRC-RL model architecture takes its inspiration from the original CURL implementation by Laskin et al. [10]. The original model is extended by incorporating additional decoder and feature predictor to facilitate computing the CRC loss function as described in the previous section. The model is implemented using PyTorch [57] deep learning framework. The reinforcement learning framework for policy estimation makes use of the publicly released implementation of the SAC algorithm by Yarats et al. [58]. The query encoder and decoder architecture is similar to the ones used in the above work. The query encoder weights are tied between the actor and critic

Table 1: Hyper-parameters used for DMControl experiments. Most hyper-parameters values are unchanged across environments with the exception for action repeat, learning rate, and batch size.

Hyper-parameter	Value
Pre transform image size	(100, 100)
Image size	(84, 84)
Action repeat	8
Frame stack	3
Transform	Random crop
Replay buffer capacity	100000
Initial steps	1000
Batch size	512
Hidden layers	1024
Evaluation episodes	10
Optimizer	Adam
Learning rate ($f_\theta, \pi_\psi, Q_\phi$)	1e-3
Learning rate (α)	1e-4
Critic target update frequency	2
Convolution layers	4
Number of filters	32
Latent dimension	50
Discount (γ)	0.99
Initial temperature	0.1

so that they both use the same encoder to embed input image observations. The feature predictor module is a MLP network which consists of cascaded linear layers and ReLU activation function. The complete list of hyper-parameters is shown in Table 1. A number of experiments are carried out to establish the efficacy of the proposed model. The design choices are justified through several ablation studies as discussed below.

3.1 Performance Comparison

The performance of the proposed CRC-RL model is compared with the current state-of-the-art methods on the challenging Deep mind control suite (DMControl) environments [29]. The outcome is shown in Table 2 and 3 after training for 100K and 500K environment steps respectively. It can be observed that the proposed CRC-RL model outperforms the current state-of-the-art methods, such as CURL [10], SODA [23], PlaNet [59], Dreamer [60], SAC+AE [17], pixel-based SAC [45] on most of the DMControl environments, thereby establishing the superiority of our approach. The environments shown in Table 3 are difficult compared to those shown in Table 2 and hence require longer training time. In this case, our proposed model outperforms the baseline CURL model in only 300K training steps.

Table 2: Mean episodic reward (with standard deviation) over 10 evaluation runs on DMControl environments after training for 100k environment steps. The best scores are shown in bold letters.

100K Step Scores	Our Method	CURL [10]	SODA [23]	PLANET [59]	DREAMER [60]	SAC+AE [17]	PIXEL SAC [45]	STATE SAC [45]	% Increase over CURL
FINGER, SPIN	793±36	767±56	363±185	136±216	341±70	740±64	179±66	811±46	3.38
CARTPOLE, SWINGUP	813±45	582±146	474±143	297±39	326±27	311±11	419±40	835±22	39.6
REACHER, EASY	636±301	538±233	-	20±50	314±155	274±14	145±30	746±25	18.2
CHEETAH, RUN	355±31	299±48	-	138±88	235±137	267±24	197±15	616±18	18.7
WALKER, WALK	490±52	403±24	635±48	224±48	277±12	394±22	42±12	891±82	21.5
BALL IN CUP, CATCH	832±81	769±43	539±111	0±0	246±174	391±82	312±63	746±91	8.19

Table 3: Mean episodic score (with standard deviation) for 10 evaluation runs on DMControl environments obtained after training for 500k environment steps. The best scores are shown in bold letters.

Environment	Our Method*	CURL	% Increase over CURL
QUADRUPED, WALK	88 ± 51	39±22	125.6
HOPPER, HOP	61 ± 33	10±17	510
WALKER, RUN	306 ± 5	245±32	24.8
FINGER TURN, HARD	423 ± 78	207±32	104.3

* shows values for 300K training steps

3.2 t-SNE Visualizations

To better understand the relationship between the learned latent representations and the action generated by the RL policy, we generate the two-dimensional t-SNE plots of feature embeddings obtained from the query encoder for 3 different environments as shown in Figure 2. These features are assigned with the corresponding action labels generated by partitioning the action space into five clusters by using the k-mean clustering algorithm. As one can observe, the proposed CRC-RL model leads to more pristine clusters with lesser outliers compared to the baseline CURL [10] algorithm for some amount of training. Compared to the Cartpole environment, other two are comparatively more complex and require larger amount of time for training. This shows that the proposed model leads to better correlation between the feature embeddings and agent actions. This aspect has not been empirically investigated extensively in the existing literature and thus, the current work makes a novel contribution by filling this void.

3.3 Feature Correlation Heat Maps

Another study is performed to validate our hypothesis that the proposed CRC loss contribute new information resulting in learning new feature representations which are distinct from those obtained using individual losses. In this study, the correlation matrices between the latent features obtained with the baseline CURL algorithm (that uses contrastive loss) and that with the proposed CRC-RL model (that uses CRC loss) is plotted as heat-maps as shown in Figure 4. These matrices are generated by collecting 200 sample embeddings from both models trained with 49000

environment steps. Since, each image sample is encoded into a 50×1 feature vector, the features generated by the above two methods are grouped into two feature matrices (say, F_1 and F_2) of size 200×50 . The correlation between these two feature matrices results in a 400×400 matrix is visualized as a heat map in the above figure where the darker regions shows higher correlation and lighter regions show lower correlation. It is observed that off-diagonal regions have lower correlation (lighter regions) indicating that the two feature embeddings (F_1 and F_2) are very distinct from each other. The diagonal regions are highly correlated (darker regions) as they correspond to the features from the same method. Another interesting finding of this study is that these heat maps show increasingly complex patterns for difficult environments such as 'Walker-walk' or 'Cheetah-Run' compared to simpler environments such as 'Cartpole-Swingup'. These patterns evolve over time and stabilize as the training performance saturates. This is an interesting insight that may provide clue to better understand the relationship between features and action policies learned in an end-to-end RL framework.

3.4 Ablation Study

Three separate ablation studies are carried out to justify the design choices made in this paper as described below.

3.4.1 Usefulness of CRC loss function

First study validates the usefulness of the proposed CRC loss function comprising of contrastive, reconstruction and consistency losses. The outcome is shown in Figure 3. We start with the baseline CURL model [10] that uses contrastive loss to learn the feature presentations. Then this model is trained with a combined loss function of contrastive and reconstruction loss and finally, with the CRC loss function comprising of contrastive, reconstruction and consistency losses. The inclusion of these losses require modifying the existing CURL model leading to the formation of the CRC-RL model proposed in this paper. The figure shows that CRC-RL performs better than the other two for the benchmark problems from the Deepmind control suite (DMC), namely, 'Cheetah-Run' or 'Walker-

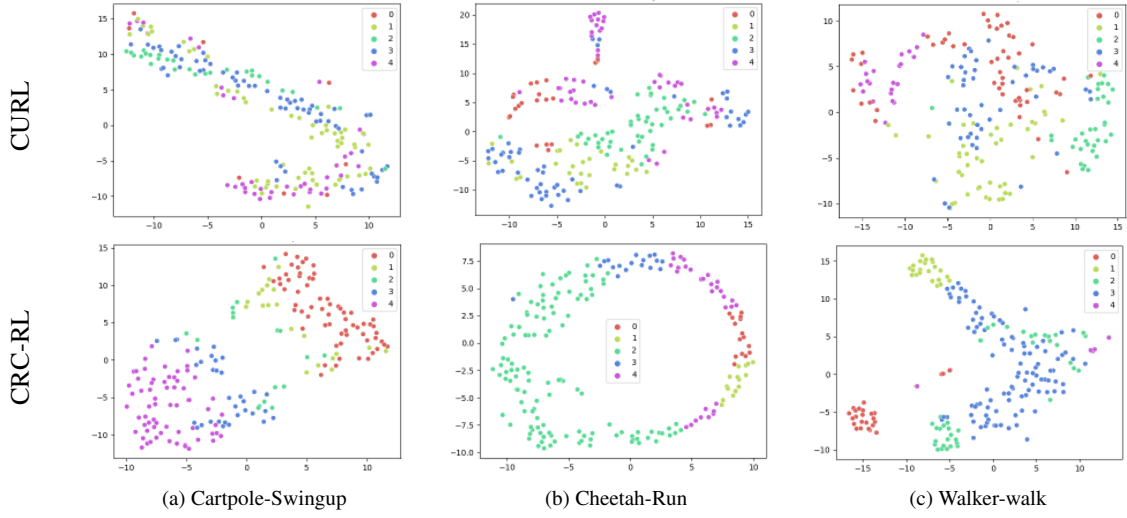


Figure 2: t-SNE visualization of latent feature embeddings obtained from query encoder at 49K training steps. Colors correspond to cluster labels in the action space. One can observe that CRC-RL leads to more pristine clusters with less outliers compared to CURL.

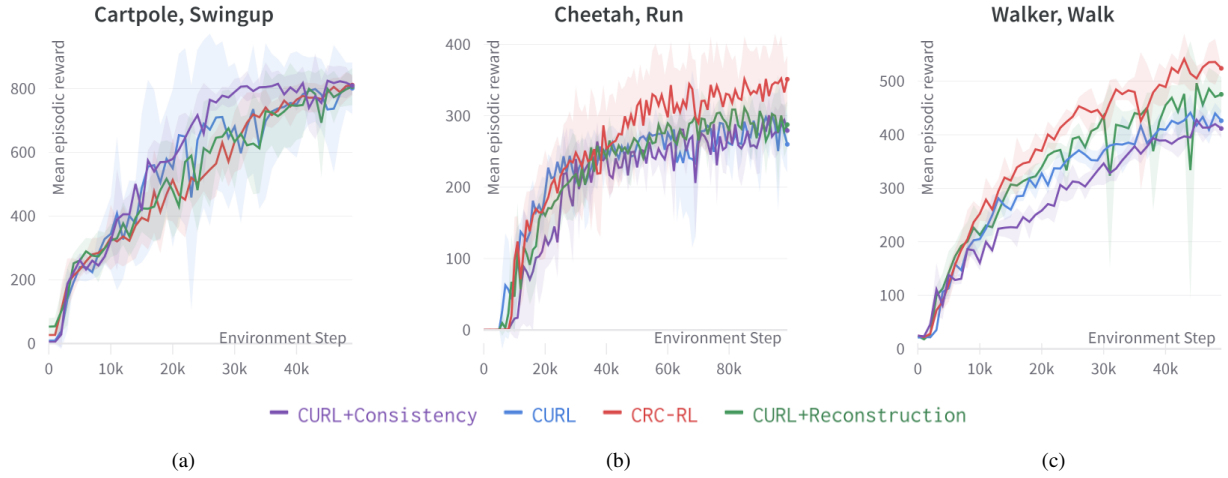


Figure 3: Effect of incorporating various loss components. CRC loss function performs better than other combinations for more difficult environments such as 'Cheetah-Run' and 'Walker-walk'.

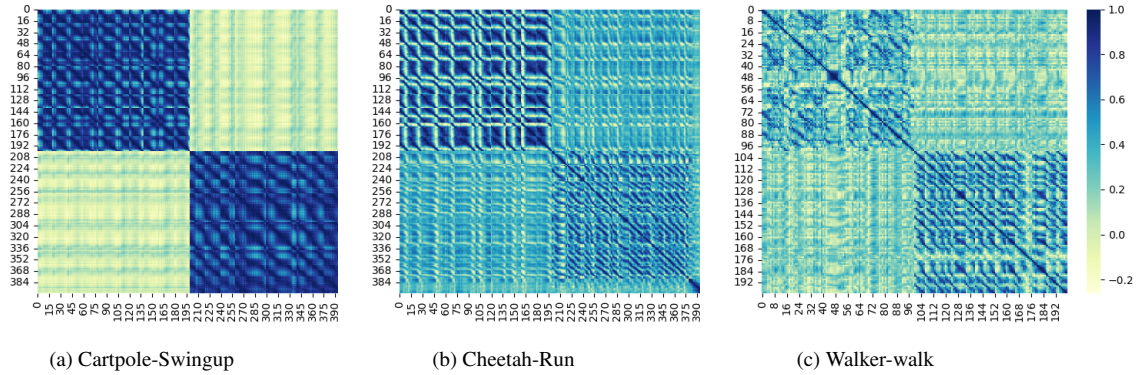


Figure 4: Feature correlation heat-maps for three environments showing the correlation between the latent features obtained with CURL and CRC-RL models. The models are trained for 49K environment steps and 200 latent features are used to generate this plot.

walk’. These two are comparatively difficult problems to solve compared to simpler problems such as the ‘Cartpole-Swingup’ problem which does not benefit from the proposed CRC-RL model. This observation clearly establishes the usefulness of the proposed approach. This becomes more evident in the second ablation study discussed in the next section below.

3.4.2 Relative weights of loss components in the CRC loss function

In this study, the relative weights of three loss components, namely, contrastive, reconstruction and consistency loss, are varied and its effect on the validation performance is compared as shown in Figure 5. The weights are varied with the constraint of forming a convex sum. In other words, $c_i > 0, i \in 1, 2, 3$ and $\sum_i c_i = 1$. The figure shows that the individual loss functions do not always provide the best performance. The best performance is obtained by a combination of all the three losses. Having equal weights ($c_1 = c_2 = c_3 = 0.33$) for all the three losses have a regularizing effect on model performance in the sense that the performance is traded for better generalizability. This is evident from the fact that the validation performance curve with this combination of weights lie somewhere in the middle of the all the curves. The generalization capability of the proposed model is demonstrated in the third ablation study discussed next.

3.4.3 Generalization Capability of the CRC-RL model

In order to test the generalization capabilities of the proposed CRC-RL model, another experiment is performed where the RL models are trained on images augmented with *random crop* effect and then validated on images augmented with *Video-Easy* and *Color-Hard* artifacts [23]. The outcome is shown in Figure 6. Comparing with the validation

plots in Figure 5, it is observed that the overall performance has come down significantly due to these complex augmentations which makes it difficult for the model to generalize when trained only with images augmented with only *random crop* artefact. However, even in this case, the RL model trained with CRC loss function provides the best or closer-to-the-best evaluation performance compared to the models that use individual loss components for training. This demonstrates the superior generalization capability of the proposed CRC-RL model over the existing models that use one of the above loss functions for training. It also corroborates the earlier finding mentioned in the previous subsection that the equal weights for individual loss components in the CRC loss function have a regularizing effect on the model performance.

4 Conclusions

The paper addresses the problem of feature representation learning in end-to-end reinforcement learning models with visual observations. Specifically, a new loss function, called CRC loss, is proposed to learn action-dependent features leading to superior performance in learning optimal action policies. This loss function is a combination of three different loss functions, namely, the image reconstruction loss, the contrastive loss and the consistency loss. Through empirical analysis including latent feature visualization, an attempt is made to generate new insights that can better explain the relationship between the features being learnt and the actions being taken by the RL agent. The resulting architecture is shown to outperform the existing state-of-the-art methods in solving the challenging DMC problems by a significant margin thereby forming a new benchmark in this field. The future work will involve carrying out more in-depth analysis and evaluation of the individual loss components on the overall performance as well as on the quality

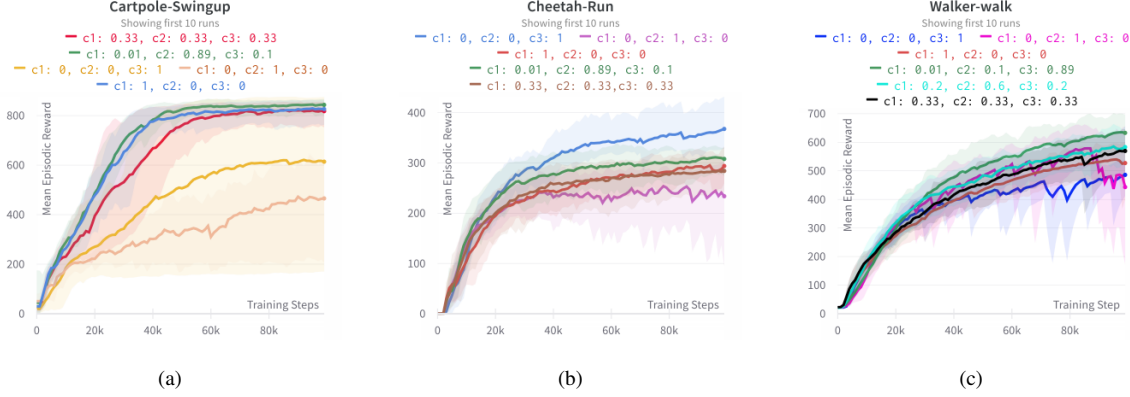


Figure 5: Effect of varying weighting parameters for different loss functions on the Evaluation performance. c_1 , c_2 and c_3 are the weights to the contrastive loss, the reconstruction loss and the consistency loss respectively in the CRC loss function. The environments used are: (a) Cartpole-Swingup, (b) Cheetah-Run and (c) Walker-walk. Varying these parameters have a regularizing effect on the training performance. A smoothing factor of 0.5 is applied to the plot.

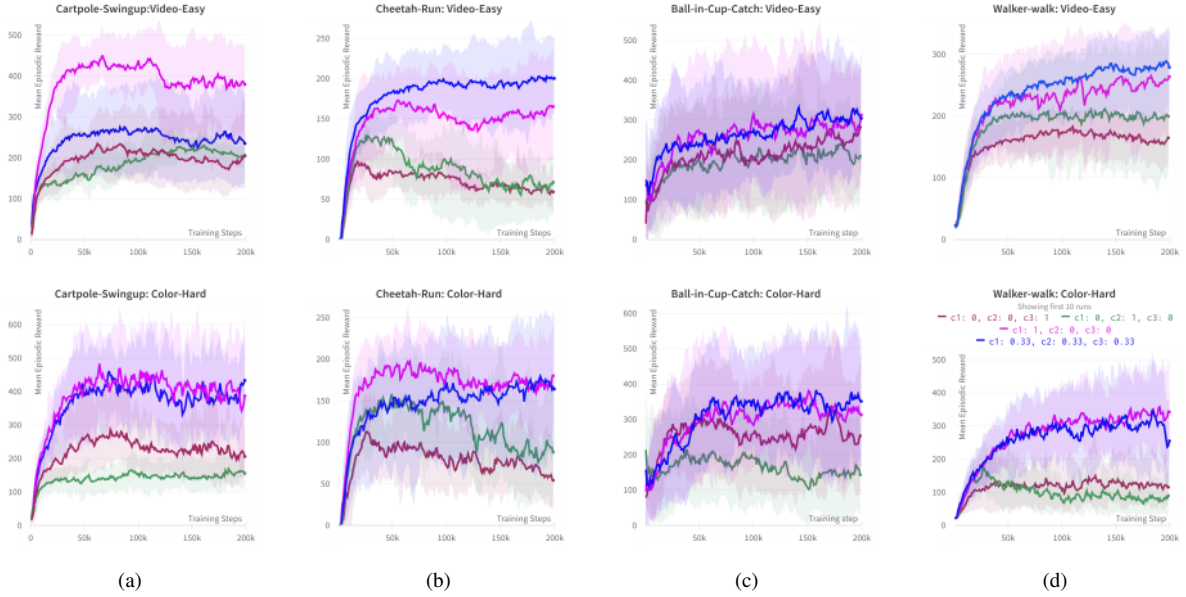


Figure 6: Generalization capabilities of CRC-RL algorithm. c_1 , c_2 and c_3 are the weights to the contrastive loss, the reconstruction loss and the consistency loss respectively in the CRC loss function. The environments used are: (a) Cartpole-Swingup, (b) Cheetah-Run and (c) Ball-in-Cup-Catch and (d) Walker-walk. The RL models are trained on images with *random-crop* augmentation and evaluated on images with *Video-Easy* and *Color-Hard* augmentations. Compared to the individual losses, CRC loss provide best or second-best evaluation performance for these new augmentations thereby establishing the superior generalization capabilities of the CRC-RL model.

of features being learned.

References

- [1] Volodymyr Mnih, Koray Kavukcuoglu, David Silver, Andrei A Rusu, Joel Veness, Marc G Bellemare, Alex Graves, Martin Riedmiller, Andreas K Fidjeland, Georg Ostrovski, et al. Human-level control through deep reinforcement learning. *nature*, 518(7540):529–533, 2015.
- [2] Shan Xue, Biao Luo, Derong Liu, and Ying Gao. Event-triggered integral reinforcement learning for nonzero-sum games with asymmetric input saturation. *Neural Networks*, 152:212–223, 2022.
- [3] Sergey Levine, Chelsea Finn, Trevor Darrell, and Pieter Abbeel. End-to-end training of deep visuomotor policies. *The Journal of Machine Learning Research*, 17(1):1334–1373, 2016.
- [4] Ahmed Hussain Qureshi, Yutaka Nakamura, Yuichiro Yoshikawa, and Hiroshi Ishiguro. Intrinsically motivated reinforcement learning for human–robot interaction in the real-world. *Neural Networks*, 107:23–33, 2018.
- [5] Jiexin Wang, Stefan Elfving, and Eiji Uchibe. Modular deep reinforcement learning from reward and punishment for robot navigation. *Neural Networks*, 135:115–126, 2021.
- [6] Yutaka Nakamura, Takeshi Mori, Masa-aki Sato, and Shin Ishii. Reinforcement learning for a biped robot based on a cpg-actor-critic method. *Neural networks*, 20(6):723–735, 2007.
- [7] Wei Yang, Xiaolong Wang, Ali Farhadi, Abhinav Gupta, and Roozbeh Mottaghi. Visual semantic navigation using scene priors. *arXiv preprint arXiv:1810.06543*, 2018.
- [8] Yuke Zhu, Roozbeh Mottaghi, Eric Kolve, Joseph J Lim, Abhinav Gupta, Li Fei-Fei, and Ali Farhadi. Target-driven visual navigation in indoor scenes using deep reinforcement learning. In *2017 IEEE international conference on robotics and automation (ICRA)*, pages 3357–3364. IEEE, 2017.
- [9] Misha Laskin, Kimin Lee, Adam Stooke, Lerrel Pinto, Pieter Abbeel, and Aravind Srinivas. Reinforcement learning with augmented data. *Advances in neural information processing systems*, 33:19884–19895, 2020.
- [10] Michael Laskin, Aravind Srinivas, and Pieter Abbeel. Curl: Contrastive unsupervised representations for reinforcement learning. In *International Conference on Machine Learning*, pages 5639–5650. PMLR, 2020.
- [11] Fuzhen Zhuang, Zhiyuan Qi, Keyu Duan, Dongbo Xi, Yongchun Zhu, Hengshu Zhu, Hui Xiong, and Qing He. A comprehensive survey on transfer learning. *Proceedings of the IEEE*, 109(1):43–76, 2020.
- [12] Tariqul Islam, Dm Mehedi Hasan Abid, Tanvir Rahman, Zahura Zaman, Kausar Mia, and Ramim Hossain. Transfer learning in deep reinforcement learning. In *Proceedings of Seventh International Congress on Information and Communication Technology: ICICT 2022, London, Volume 1*, pages 145–153. Springer, 2022.
- [13] Yesmina Jaafra, Jean Luc Laurent, Aline Deruyver, and Mohamed Saber Naceur. A review of meta-reinforcement learning for deep neural networks architecture search. *arXiv preprint arXiv:1812.07995*, 2018.
- [14] Timothy Hospedales, Antreas Antoniou, Paul Micaelli, and Amos Storkey. Meta-learning in neural networks: A survey. *IEEE transactions on pattern analysis and machine intelligence*, 44(9):5149–5169, 2021.
- [15] Burr Settles. Active learning literature survey. 2009.
- [16] Yoshua Bengio, Aaron Courville, and Pascal Vincent. Representation learning: A review and new perspectives. *IEEE transactions on pattern analysis and machine intelligence*, 35(8):1798–1828, 2013.
- [17] Denis Yarats, Amy Zhang, Ilya Kostrikov, Brandon Amos, Joelle Pineau, and Rob Fergus. Improving sample efficiency in model-free reinforcement learning from images. In *Proceedings of the AAAI Conference on Artificial Intelligence*, volume 35, pages 10674–10681, 2021.
- [18] Linus Ericsson, Henry Gouk, Chen Change Loy, and Timothy M Hospedales. Self-supervised representation learning: Introduction, advances, and challenges. *IEEE Signal Processing Magazine*, 39(3):42–62, 2022.
- [19] Dor Bank, Noam Koenigstein, and Raja Giryes. Autoencoders. *arXiv preprint arXiv:2003.05991*, 2020.
- [20] Daoyu Lin, Kun Fu, Yang Wang, Guangluan Xu, and Xian Sun. Marta gans: Unsupervised representation learning for remote sensing image classification. *IEEE Geoscience and Remote Sensing Letters*, 14(11):2092–2096, 2017.
- [21] Yuxin Peng and Jinwei Qi. Cm-gans: Cross-modal generative adversarial networks for common representation learning. *ACM Transactions on Multimedia Computing, Communications, and Applications (TOMM)*, 15(1):1–24, 2019.
- [22] Ting Chen, Simon Kornblith, Mohammad Norouzi, and Geoffrey Hinton. A simple framework for contrastive learning of visual representations. In *International conference on machine learning*, pages 1597–1607. PMLR, 2020.
- [23] Nicklas Hansen and Xiaolong Wang. Generalization in reinforcement learning by soft data augmentation. In *2021 IEEE International Conference on Robotics and Automation (ICRA)*, pages 13611–13617. IEEE, 2021.
- [24] Chelsea Finn, Xin Yu Tan, Yan Duan, Trevor Darrell, Sergey Levine, and Pieter Abbeel. Learning visual feature spaces for robotic manipulation with deep spatial autoencoders. *arXiv preprint arXiv:1509.06113*, 25:2, 2015.
- [25] Adam Stooke, Kimin Lee, Pieter Abbeel, and Michael Laskin. Decoupling representation learning from reinforcement learning. In *International Conference on Machine Learning*, pages 9870–9879. PMLR, 2021.
- [26] Max Jaderberg, Volodymyr Mnih, Wojciech Marian Czarnecki, Tom Schaul, Joel Z Leibo, David Silver, and Koray Kavukcuoglu. Reinforcement learning with unsupervised auxiliary tasks. *arXiv preprint arXiv:1611.05397*, 2016.

- [27] Konstantia Xenou, Georgios Chalkiadakis, and Stergos Afantenos. Deep reinforcement learning in strategic board game environments. In *European Conference on Multi-Agent Systems*, pages 233–248. Springer, 2018.
- [28] Behnam Neyshabur, Stephen Tu, Xingyou Song, Yiding Jiang, and Yilun Du. Observational overfitting in reinforcement learning. 2020.
- [29] Yuval Tassa, Yotam Doron, Alistair Muldal, Tom Erez, Yazhe Li, Diego de Las Casas, David Budden, Abbas Abdolmaleki, Josh Merel, Andrew Lefrancq, et al. Deepmind control suite. *arXiv preprint arXiv:1801.00690*, 2018.
- [30] Richard S Sutton and Andrew G Barto. *Reinforcement learning: An introduction*. MIT press, 2018.
- [31] Andrew G Barto. Reinforcement learning and dynamic programming. In *Analysis, Design and Evaluation of Man-Machine Systems 1995*, pages 407–412. Elsevier, 1995.
- [32] Hado Van Hasselt, Arthur Guez, and David Silver. Deep reinforcement learning with double q-learning. In *Proceedings of the AAAI Conference on Artificial Intelligence*, volume 30, 2016.
- [33] Mohit Sewak. Deep q network (dqn), double dqn, and dueling dqn. In *Deep Reinforcement Learning*, pages 95–108. Springer, 2019.
- [34] Volodymyr Mnih, Koray Kavukcuoglu, David Silver, Alex Graves, Ioannis Antonoglou, Daan Wierstra, and Martin Riedmiller. Playing atari with deep reinforcement learning. *arXiv preprint arXiv:1312.5602*, 2013.
- [35] Sean D Holcomb, William K Porter, Shaun V Ault, Guifen Mao, and Jin Wang. Overview on deepmind and its alphago zero ai. In *Proceedings of the 2018 international conference on big data and education*, pages 67–71, 2018.
- [36] Kai Arulkumaran, Marc Peter Deisenroth, Miles Brundage, and Anil Anthony Bharath. Deep reinforcement learning: A brief survey. *IEEE Signal Processing Magazine*, 34(6):26–38, 2017.
- [37] Timothy P Lillicrap, Jonathan J Hunt, Alexander Pritzel, Nicolas Heess, Tom Erez, Yuval Tassa, David Silver, and Daan Wierstra. Continuous control with deep reinforcement learning. *arXiv preprint arXiv:1509.02971*, 2015.
- [38] Yan Duan, Xi Chen, Rein Houthoofd, John Schulman, and Pieter Abbeel. Benchmarking deep reinforcement learning for continuous control. In *International conference on machine learning*, pages 1329–1338. PMLR, 2016.
- [39] Shixiang Gu, Ethan Holly, Timothy Lillicrap, and Sergey Levine. Deep reinforcement learning for robotic manipulation with asynchronous off-policy updates. In *2017 IEEE international conference on robotics and automation (ICRA)*, pages 3389–3396. IEEE, 2017.
- [40] Hai Nguyen and Hung La. Review of deep reinforcement learning for robot manipulation. In *2019 Third IEEE International Conference on Robotic Computing (IRC)*, pages 590–595. IEEE, 2019.
- [41] Deirdre Quillen, Eric Jang, Ofir Nachum, Chelsea Finn, Julian Ibarz, and Sergey Levine. Deep reinforcement learning for vision-based robotic grasping: A simulated comparative evaluation of off-policy methods. In *2018 IEEE International Conference on Robotics and Automation (ICRA)*, pages 6284–6291. IEEE, 2018.
- [42] Shirin Joshi, Sulabh Kumra, and Ferat Sahin. Robotic grasping using deep reinforcement learning. In *2020 IEEE 16th International Conference on Automation Science and Engineering (CASE)*, pages 1461–1466. IEEE, 2020.
- [43] Pengyu Yue, Jing Xin, Huan Zhao, Ding Liu, Mao Shan, and Jian Zhang. Experimental research on deep reinforcement learning in autonomous navigation of mobile robot. In *2019 14th IEEE Conference on Industrial Electronics and Applications (ICIEA)*, pages 1612–1616. IEEE, 2019.
- [44] Volodymyr Mnih, Adria Puigdomenech Badia, Mehdi Mirza, Alex Graves, Timothy Lillicrap, Tim Harley, David Silver, and Koray Kavukcuoglu. Asynchronous methods for deep reinforcement learning. In *International conference on machine learning*, pages 1928–1937. PMLR, 2016.
- [45] Tuomas Haarnoja, Aurick Zhou, Kristian Hartikainen, George Tucker, Sehoon Ha, Jie Tan, Vikash Kumar, Henry Zhu, Abhishek Gupta, Pieter Abbeel, et al. Soft actor-critic algorithms and applications. *arXiv preprint arXiv:1812.05905*, 2018.
- [46] John Schulman, Filip Wolski, Prafulla Dhariwal, Alec Radford, and Oleg Klimov. Proximal policy optimization algorithms. *arXiv preprint arXiv:1707.06347*, 2017.
- [47] Nicolò Botteghi, Mannes Poel, and Christoph Brune. Unsupervised representation learning in deep reinforcement learning: A review. *arXiv preprint arXiv:2208.14226*, 2022.
- [48] Walter Hugo Lopez Pinaya, Sandra Vieira, Rafael Garcia-Dias, and Andrea Mechelli. Autoencoders. In *Machine learning*, pages 193–208. Elsevier, 2020.
- [49] Antonin Raffin, Ashley Hill, René Traoré, Timothée Lesort, Natalia Díaz-Rodríguez, and David Filliat. S-rl toolbox: Environments, datasets and evaluation metrics for state representation learning. *arXiv preprint arXiv:1809.09369*, 2018.
- [50] Sascha Lange and Martin Riedmiller. Deep auto-encoder neural networks in reinforcement learning. In *The 2010 international joint conference on neural networks (IJCNN)*, pages 1–8. IEEE, 2010.
- [51] Alexander Kolesnikov, Xiaohua Zhai, and Lucas Beyer. Revisiting self-supervised visual representation learning. In *Proceedings of the IEEE/CVF conference on computer vision and pattern recognition*, pages 1920–1929, 2019.
- [52] Roberta Raileanu, Max Goldstein, Denis Yarats, Ilya Kostrikov, and Rob Fergus. Automatic data augmentation for generalization in deep reinforcement learning. *arXiv preprint arXiv:2006.12862*, 2020.
- [53] Wenling Shang, Xiaofei Wang, Aravind Srinivas, Aravind Rajeswaran, Yang Gao, Pieter Abbeel, and Misha Laskin. Reinforcement learning with latent flow. *Advances in Neural Information Processing Systems*, 34:22171–22183, 2021.

- [54] Olivier Henaff. Data-efficient image recognition with contrastive predictive coding. In *International conference on machine learning*, pages 4182–4192. PMLR, 2020.
- [55] Aaron van den Oord, Yazhe Li, and Oriol Vinyals. Representation learning with contrastive predictive coding. *arXiv preprint arXiv:1807.03748*, 2018.
- [56] Partha Ghosh, Mehdi SM Sajjadi, Antonio Vergari, Michael Black, and Bernhard Schölkopf. From variational to deterministic autoencoders. *arXiv preprint arXiv:1903.12436*, 2019.
- [57] Adam Paszke, Sam Gross, Francisco Massa, Adam Lerer, James Bradbury, Gregory Chanan, Trevor Killeen, Zeming Lin, Natalia Gimelshein, Luca Antiga, et al. Pytorch: An imperative style, high-performance deep learning library. *Advances in neural information processing systems*, 32, 2019.
- [58] Denis Yarats, Ilya Kostrikov, and Rob Fergus. Image augmentation is all you need: Regularizing deep reinforcement learning from pixels. In *International Conference on Learning Representations*, 2020.
- [59] Danijar Hafner, Timothy Lillicrap, Ian Fischer, Ruben Villegas, David Ha, Honglak Lee, and James Davidson. Learning latent dynamics for planning from pixels. In *International conference on machine learning*, pages 2555–2565. PMLR, 2019.
- [60] Danijar Hafner, Timothy Lillicrap, Jimmy Ba, and Mohammad Norouzi. Dream to control: Learning behaviors by latent imagination. *arXiv preprint arXiv:1912.01603*, 2019.